

Enhanced near-field imaging contrasts of silver nanoparticles by localized surface plasmon

Yun-Chorng Chang*, Hsueh-Wei Chen, and Shih-Hui Chang

Institute of Electro-Optical Science and Engineering, National Cheng Kung University

ychang6@mail.ncku.edu.tw

IEEE Journal of Selected Topics in Quantum Electronics VO.14 , ISSUE 6 ,PP.1536-1539 ,NOV-DEC 2008

Techniques of nanoparticle detection have improved significantly for the demands of unprecedented high resolution in nanotechnologies. Information about the spatial distribution and chemical identity of nanoparticles provide vital information for both nano- and bio-sciences. Near-field imaging techniques with sub-wavelength spatial resolution offer fast, non-invasive and highly sensitive detections for wide variety of materials [Refs. 1-4]. A scattering type near-field scanning optical microscopy (NSOM) [Ref. 5] is also demonstrated to be able to distinguish particle made from different materials with with sub-10 nm resolution.



In our previous work, near-field images of Ag nanoparticles are studied using a near-field optical microscopy operating at illumination mode with blue, green and red probing lights [Ref. 6]. The obtained far field intensity contrast between the nanoparticle and background strongly depends on the sizes of nanoparticles and the wavelength of probing light. Experimental NSOM images supported by theoretical 3-dimensional finite-difference-time-domain simulation demonstrate that the intensity contrast is enhanced at wavelength close to the localized surface plasmon resonance (LSPR) peak of the nanoparticle. The abilities to distinguish nanoparticles with different LSPR properties on the same substrate can lead to a material-specific NSOM imaging technique.

Fabrications of Ag nanoparticle arrays were achieved by annealing 5 nm and 10 nm Ag thin films at 600 ° C for 30 minute inside a nitrogen-flowing oven. Double-side-polished quartz substrates or silicon substrates were used for different subsequent analyses. Ag nanoparticles fabricated on top of silicon substrates were analyzed by a scanning electron microscopy (SEM). Fig 1(a) and 1(b) were SEM images of the Ag nanoparticles fabricated from 5 nm and 10 nm of Ag thin film on top of silicon substrates, respectively. The size distributions of Ag nanoparticles were subsequently analyzed from the SEM images and the results were shown in Fig. 1(c). The size and its variation are larger for Ag nanoparticles fabricated from thicker films. A commercial UV-VIS absorption spectrophotometer (Hitachi U-3010) was used to determine the surface plasmon resonance of the Ag nanoparticles, shown in Fig. 1(d). Samples for the absorption measurements were grown on top of transparent quartz substrates. The absorption spectrum from the Ag nanoparticles fabricated from 5 nm film, curve (a), exhibits an absorption peak centered at 440 nm.

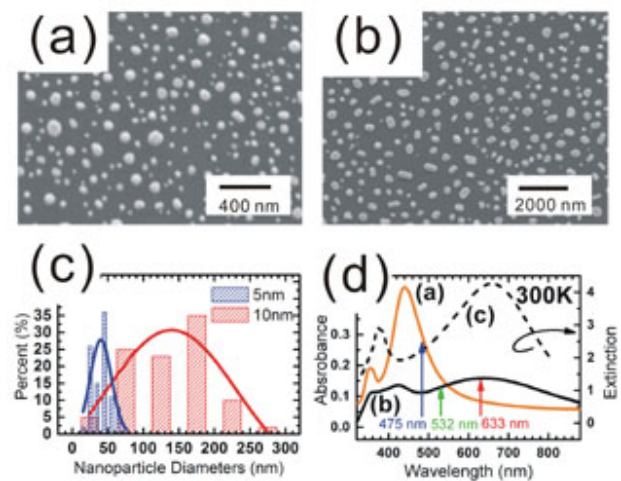


Fig 1 SEM micrographs of (a) 5 nm and (b) 10 nm of Ag thin films annealed at 600 ° C for 30 minutes. (c) Distributions of Ag nanoparticle diameters and (d) absorption spectra for nanoparticles fabricated from 5 nm (curve a) and 10 nm (curve b) thin films. Curve c represents the calculated extinction spectrum for a 160 nm Ag nanoparticle from FDTD simulation. The blue, green, and red arrows in (d) indicates the laser

This peak is referred as the scattering peak from the Ag nanoparticles. Curve (b) is the absorption spectrum measured from Ag nanoparticles fabricated from 10 nm films and two peaks centered at 420 nm and 630 nm are corresponding to the absorption and scattering peaks, respectively. The blue, green, and red arrows shown in Fig. 1(d) are the laser wavelength used in the subsequent near field measurements.

A commercial near-field scanning optical microscope scanner (Veeco Aurora-3) was used to obtain the near field images of the Ag nanoparticles. The probe tip was a tapered single mode fiber with an 80 nm aperture coated with 100 nm aluminum. Emission from a He-Ne laser ($\lambda = 633$ nm) or frequency-doubled solid state lasers ($\lambda = 475$ nm or 532 nm) was coupled into the other end of the tapered fiber. The NSOM was operated under the illumination mode and the transmitted light was collected in the far field by a microscope objective and analyzed by a photomultiplier.

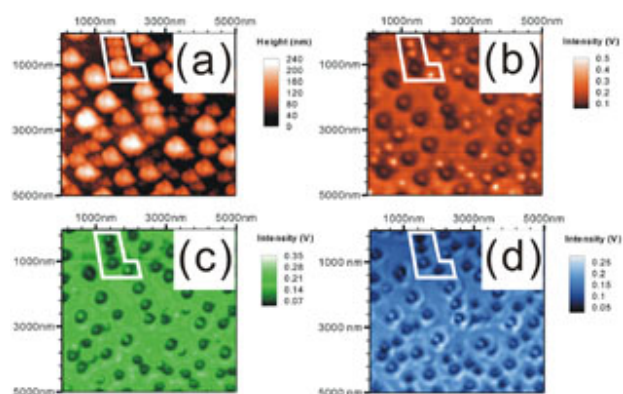


Fig. 2 (a) AFM image and NSOM images taken by using (b) 633 nm, (c) 532 nm, and (d) 475 nm laser light, of Ag nanoparticle fabricated by annealing 10 nm Ag thin film.

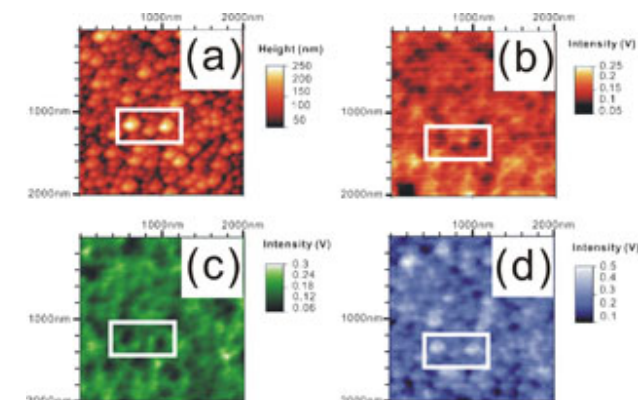


Fig. 3 (a) AFM image and NSOM images taken by using (b) 633 nm, (c) 532 nm, and (d) 475 nm laser light, of Ag nanoparticle fabricated by annealing 5 nm Ag thin film.

NSOM images of Ag nanoparticles fabricated from 10 nm thin films are shown in Fig. 2. The topography image of the sample is shown in Fig. 2(a), and the NSOM images using 633 nm, 532 nm, and 475 nm laser light are shown in Fig. 2(b), (c), and (d), respectively. It should be noted that these lasers were with different emission intensities, and comparisons of the absolute transmitted intensities between different lasers were irrelevant. Only the intensity contrast between the signal from the nanoparticle and the background was discussed. Four nanoparticles are observed inside a high-lighted polygon area in Fig 2(a) and one particle is clearly larger than the other three. These three smaller nanoparticles exhibited a higher transmitted intensity contrast when using 633 nm laser, shown in Fig. 2(b). The transmitted intensity contrast became smaller when using 532 nm laser and became the smallest when using 475 nm laser. The decrease in intensity contrast with decreasing excitation wavelength matched the trend shown in the spectrum range between 475 nm and 633 nm of curve (b) in Fig. 1(d). The intensity contrast was the highest when the excitation wavelength was close to the surface plasmon resonance of the Ag nanoparticles. Similar NSOM images of Ag nanoparticles fabricated from 5 nm thin film are shown in Fig. 3. A rectangular area is also high-lighted and three nanoparticles are observed inside this area. The size of the middle nanoparticle is smaller than the other two. NSOM images with different lasers are shown in Fig. 3(b), (c), and (d). These two nanoparticles on the side exhibited the highest intensity contrast when using 475 nm laser. The contrast became smaller with increasing excitation laser wavelength. The decrease in intensity contrast with increasing excitation wavelength matched the trend shown in curve (a) in Fig. 1(d).

From the results shown in Figs. 2 and 3, the intensity contrast for the same Ag nanoparticle depends strongly on the excitation wavelength. The contrast becomes higher when the excitation wavelength is closer to the surface plasmon resonance. For larger Ag nanoparticles, fabricated from 10 nm thin films, the surface plasmon resonance wavelength

is close to 630 nm. The strong light scattering of the red laser light ($\lambda = 633$ nm) by the Ag nanoparticle results in a higher transmitted light intensity from the probe tip and a bright spot in the NSOM image. By moving away from the resonance wavelength, the light scattering becomes weaker and the transmitted light is further reduced due to the blocking by the Ag nanoparticle, which results in a dark spot in the NSOM image. For small Ag nanoparticles, fabricated from 5 nm thin films, the surface plasmon resonance shifts to close to 440 nm. Therefore, the scattering of the Ag nanoparticle is stronger when using 475 nm light and decrease with increasing wavelength. These results strongly support that surface plasmon resonance scattering can effectively increase the transmitted light intensity from the near-field probe tip. NSOM image of a Ag nanoparticle is a bright spot when the laser wavelength matches its surface plasmon resonance.

To illustrate contrast-enhanced NSOM image of a Ag nanoparticle due to localized surface plasmon resonance, a full 3D finite-difference time-domain (FDTD) simulation was carried out. A Drude-Lorentzian model for the dielectric constant of silver is given as the following

$$\varepsilon(\omega) = \varepsilon_{\infty} - \frac{\omega_D^2}{\omega^2 - j\omega\gamma_D} + \sum_{p=1}^2 \frac{\Delta\varepsilon_p \omega_p^2}{\omega_p^2 + 2j\omega\gamma_p - \omega^2}$$

where γ_D is the plasma frequency of the metal and ω_p ($p = 1, 2$) are the Lorentz resonant frequencies, and γ 's are the damping constants. These parameters were obtained by fitting with the empirical dielectric constant of bulk Ag at wavelengths from 300 nm to 800 nm [Ref. 7]. Ag nanoparticle was modeled as a hemisphere shape due to the thermal annealing process in the experiments. The extinction spectrum of a Ag nanoparticle with diameter of 160 nm on a glass substrate was calculated and was shown as the curve (c) in Fig. 1(d). It resembles the absorption spectrum measured in the experiments. To obtain the near-field scanning image of the Ag nanoparticle, a NSOM tip operated at illumination mode was included in the FDTD grid which was similar to an earlier report [Ref. 8]. The geometry of the region near the Ag nanoparticle is illustrated in Fig. 4(a). By positioning the tip at different locations around the Ag nanoparticle, the integrated far field energy flux was collected as the intensity for each pixel. Three different light sources with wavelengths at 632 nm, 532 nm, and 480 nm were used for two-dimensional scan over an area of $0.6 \mu\text{m}$ by $0.6 \mu\text{m}$ around the Ag nanoparticle. The calculated scanning NSOM images at wavelengths 632 nm, 532 nm, 480 nm were shown in Fig. 4(b), (c), and (d), respectively. The color scale was normalized by the background signal when no particle was presented and all three color bars ranged from 0.5 to 2.7. The colors of red, green, and blue were assigned as the background color with color bar value equal to 1. The FDTD results demonstrate a consistent trend that the NSOM image of the Ag nanoparticle became brighter as the probing wavelength moved toward the LSPR peak. These results are consistent with our experimental observation, which indicate that on-resonant metal nanoparticles will enhance the light extraction from the NSOM tip by a factor of at least several times. Depending on the probing light wavelength relative to the LSPR peak of the nanoparticle, the scanning images show drastically difference in contrast. This property is useful for distinguishing nanoparticles of difference sizes and is potential for

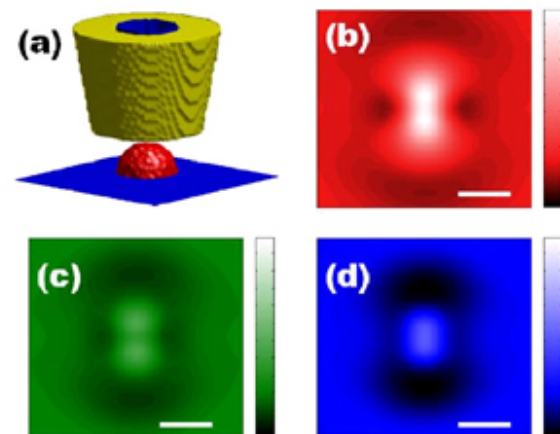


Fig 4 (a) FDTD simulation geometry shown only for the region near a Ag particle with diameter of 160 nm (b) (c) (d) FDTD collected far field intensity pattern from scanning the NSOM tip over a Ag particle at wavelength 632 nm, 532 nm, 480 nm respectively. The intensity is normalized to 1 as the case of no Ag particle. The three color bars all range from [0.5 2.7]. The scale bars indicate 160 nm.

differentiating nanoparticles of various materials.

In conclusion, Ag nanoparticles fabricated by thermal annealing of Ag thin films were studied using a near-field scanning optical microscopy (NSOM). The transmitted intensity by a NSOM operating at illumination mode was recorded when using light sources with different wavelengths. The transmitted intensity contrast between the Ag nanoparticle and the background is higher when the localized surface plasmon resonance of the Ag nanoparticle matches the wavelength of the light source. This phenomenon is theoretically confirmed by the 3-dimensional finite-difference-time-domain (FDTD) simulations. Therefore, Ag nanoparticles with controlled sizes can be distinguished by NSOM in this study, while conventional atomic force microscopy (AFM) can only recognize the existence of nanoparticles. By modifying the surface of metal nanoparticles differently according to their sizes, one can obtain a material-specific NSOM images and reveal more material information compared to the current AFM images. Further development of this technique will be beneficial for future nano-imaging of bio-molecular studies.

References:

1. U. Durug, D. W. Pohl, and F. Rohner, "Near-field optical-scanning microscopy", J. Appl. Phys., vol. 59, pp. 3318-3327, May 1986.
2. J. H. Kim, K. B. Song, "Recent progress of nano-technology with NSOM", Micron, vol. 38, pp. 409-426, 2007.
3. G. P. Wiederrecht, "Near-field optical imaging of noble metal nanoparticles", Euro. Phys J. Appl. Phys., vol. 28, pp. 3-18, Oct. 2004.
4. A. Bouhelier, "Field-enhanced scanning near-field optical microscopy", Microsc. Res. Tech., vol. 69, pp. 563-579, Jul. 2006.
5. A. Cvitkovic, N. Ocelic, and R. Hillenbrand, "Material-Specific Infrared Recognition of Single Sub-10 nm Particles by Substrate-Enhanced Scattering-Type Near-Field Microscopy", Nano Lett., vol. 7, pp. 3177-3181, Oct. 2007.
6. Y. C. Chang, H. W. Chen, and S. H. Chang, "Enhanced near-field imaging contrasts of silver nanoparticles by localized surface plasmon", IEEE Journal of Selected Topics in Quantum Electronics, vol. 14, pp. 1536-1539, Nov. 2008.
7. T. W. Lee, and S. K. Gray, "Subwavelength light bending by metal slit structures", Opt. Express, vol. 13, pp. 9652-9659, Nov. 2005.
8. S. -H. Chang, S. K. Gray, and G. C. Schatz, "Surface plasmon generation and light transmission by isolated nanoholes and arrays of nanoholes in thin metal films", Opt. Express, vol. 13, pp. 3150-3165, Apr. 2005.